Capacitive pressure sensors with stainless steel diaphragm and substrate

2004 J. Micromech. Microeng. 14 612

(http://iopscience.iop.org/0960-1317/14/4/023)

INSTITUTE OF PHYSICS PUBLISHING JOURNAL OF MICROMECHANICS AND MICROENGINEERING

J. Micromech. Microeng. **14** (2004) 612–618 PII: S0960-1317(04)70452-0

Capacitive pressure sensors with stainless steel diaphragm and substrate

Sung-Pil Chang[1] **and Mark G Allen**

Georgia Institute of Technology, School of Electrical and Computer Engineering, Atlanta, GA 30332-0250, USA

E-mail: sp.chang@samsung.com

Received 16 October 2003
Published 6 February 2004
Online at stacks.iop.org/JMM/14/612 (DOI: 10.1088/0960-1317/14/4/023)

Abstract

Much of the cost of commercial micromachined pressure sensors lies in the package that houses the device itself. If a robust material is used for the substrate of the sensors as well as the packaging material, i.e., fabricating the sensor on the package itself, cost savings for the overall system may accrue. In this work, stainless steel has been studied as a potential robust substrate and a diaphragm material for micromachined devices. Lamination process techniques combined with traditional micromachining processes have been investigated as suitable fabrication technologies. To illustrate these principles, capacitive pressure sensors based on a stainless steel diaphragm have been designed, fabricated and characterized. Each sensor uses a stainless steel substrate, a laminated stainless steel film as a suspended movable plate and a fixed, surface micromachined back electrode of electroplated nickel. The sensitivity of the device fabricated using these technologies is 9.03 ppm kPa^{-1} with a net capacitance change of 0.14 pF over a range 0–178 kPa. Two types of read-out circuitry have been introduced to microfabricated sensors for removing parasitic effects. Finally, a die-type ASIC chip was integrated and measured with this capacitive pressure. The measured value of relative voltage change was 2.85% over the applied pressure range 0–75 kPa. The sensitivity of the sensor was 0.92 mV kPa^{-1} with a gap of 21 μm.

1. Introduction

Since the root of micromachining technology is in integrated circuit processing, micromachined devices have been primarily realized using silicon substrates [1–4]. In many applications, these silicon-based devices are then protected mechanically against harsh environments by the use of a robust packaging material [5, 6]. However, this approach often leads to systems in which the cost of the package equals or exceeds the cost of the micromachined device itself. If this robust packaging material is directly used not only as the packaging or housing, but also as the substrate of the micromachined devices, many of the steps of the packaging process might be reduced, potentially leading to cost savings. Another potential advantage is that due to substrate robustness, these co-packaged devices may be used in mechanically harsh environments, such as aerospace and oceanography applications.

On the market of MEMS pressure sensors, there are two main types of pressure sensors; one type utilizes capacitive effects in sensing pressure, and the other type uses piezoresisitive effects for the same purpose [7]. Much work has been done in both areas, but there is a greater focus on capacitive pressure sensors due to certain advantages that this approach provides. Some of the advantages that it offers over the piezoresistive pressure sensor are higher measurement sensitivity, decreased temperature sensitivity, reduced power consumption and better stability [8]. These advantages portend greater potential for commercial applications. However, successful commercial exploitation of these highly miniaturized capacitive sensors is often inhibited by the presence of parasitic effects such as environmental

[1] Present address: Optical components & MEMS Lab, Central R&D Institute, Samsung Electro-Mechanics Co., Ltd, 314, Maetan3-Dong, Paldal-Gu, Suwon, Gyunggi-Do, 442-743, Korea.

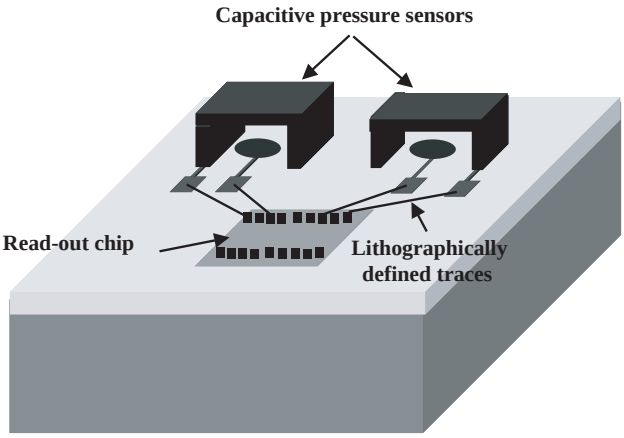

Figure 1. An example of integrated robust capacitive pressure sensors.

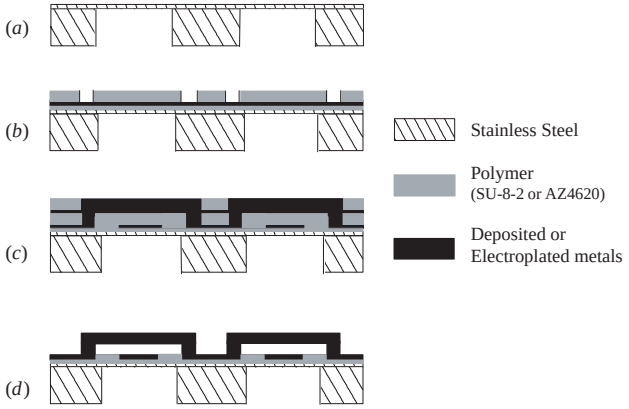

Figure 2. Fabrication sequence of pressure sensor based on stainless steel diaphragm.

noise and parasitic capacitances. Therefore, to alleviate the problems encountered in the capacitive pressure sensor approach, it is important to integrate the sensors and the circuitry as directly as possible.

For example, the capacitive pressure sensors and the read-out chip are directly integrated on the same substrate by connecting the chip to the sensors using lithographically defined traces as in figure 1. This integration allows for buffering and reduction of the parasitic effects as well as the possibility of multiplexing or conversion of capacitances to frequency or voltage.

In this work, we have investigated the use of stainless steel as a robust substrate as well as diaphragm material for suitable starting points of both bulk and surface micromachined structures. Alternative fabrication techniques, such as those commonly used in conventional machining and electronic packaging fabrication, are combined with traditional integrated-circuit-based microelectronics processing techniques to create micromachined devices on these robust substrates. An important attribute of this design is that only the stainless steel substrate and the pressure sensitive diaphragm are exposed to the environment, i.e., the sensor is self-packaged. We have also studied ways of direct integration of read-out circuitry with microfabricated sensors.

2. Fabrication process

The fabrication sequence of stainless steel diaphragm pressure sensors is shown in figure 2. The process starts on square, stainless steel substrates that are each 6.0 cm on one side, 0.8 mm thick and have a surface roughness of approximately 6–8 μm. A 6×6 array of pressure inlet holes with a diameter of 2 mm, with 7 mm center-to-center distances, is milled through the stainless steel substrates. A full hard, cold rolled stainless steel sheet type 302 (Precision Brand Product, INC) is laminated onto the milled stainless steel substrate using a hot press with a pressure of 8.65 MPa and a temperature of 175 °C for 30 min. The laminate adhesive is an epoxy-based resin designed for printed wiring board fabrication (EIS epoxy laminate prepreg no 106).

The stainless steel sheet is used as the pressure sensitive diaphragm and has a thickness of 12.7 μm and surface roughness of approximately 100 Å. Reactive ion etching (RIE) is then used to remove any exposed epoxy resin under the stainless steel diaphragm that has leaked through the pressure inlet holes (figure 2(*a*)).

A 250 Å thick titanium layer is deposited as an adhesion layer, and a 7 μm thick epoxy resist SU-8-2 (MicroChem Corp.) is deposited as an insulation layer. To create bottom electrodes, electroplating seed layers and bonding pads, Ti/Cu/Ti layers are deposited with a thickness of 250/6000/250 Å and patterned. An AZ4620 photoresist (Clariant Corp.) is spun onto the patterned layer, yielding a final thickness of photoresist of approximately 25–27 μm (figure 2(*b*)). The photoresist is patterned to create electroplating molds and nickel supports are electroplated through the molds.

To fabricate the backplate, a seed layer of Ti/Cu/Ti is deposited. A thick photoresist (AZ4620) is spun on the seed layer (approximately $\sim$25 μm thick) and patterned to form electroplating molds. These molds are then filled with nickel by electroplating (figure 2(*c*)). Finally, the photoresist sacrificial layers and the seed layers between them are etched to release the gap between the fixed backplate and the pressure sensitive stainless steel diaphragm (figure 2(*d*)). Figure 3 shows a photomicrograph of the fabricated stainless steel sensor array.

3. Theoretical model

The principle of operation is based on the pressure-induced deflection of a diaphragm and the subsequent measurement of the capacitance between this deflecting diaphragm and a fixed backplate surface micromachined over the deflecting diaphragm.

Figure 4 shows a schematic cross-section of the device, where t_g is the initial (undeflected) gap distance between the fixed back electrode and the diaphragm electrode, w_0 is the deflection at the center of the diaphragm, t_m is the thickness of the diaphragm and P is the uniform applied pressure.

For mechanical modeling, several assumptions have been made: (a) the diaphragm has isotropic mechanical properties; (b) the thickness of the metallic electrode on the plate has been neglected, since this thickness is small compared with the plate thickness; (c) electric field fringing effects have been

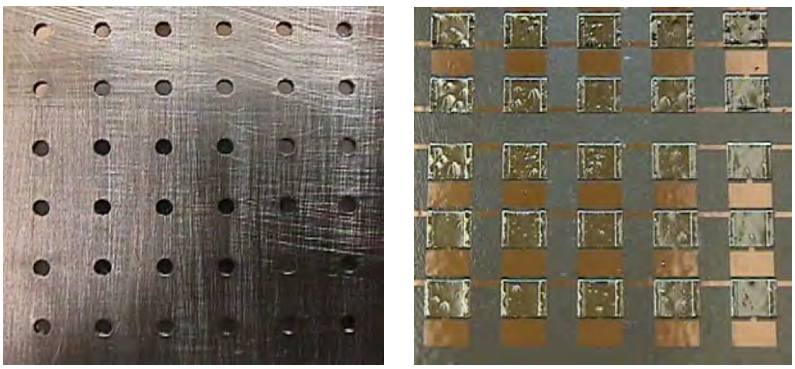

(*a*) (*b*)

Figure 3. Photomicrographs of fabricated pressure sensors. (*a*) Side exposed to environment. (*b*) Rear view showing surface micromachined backplate.

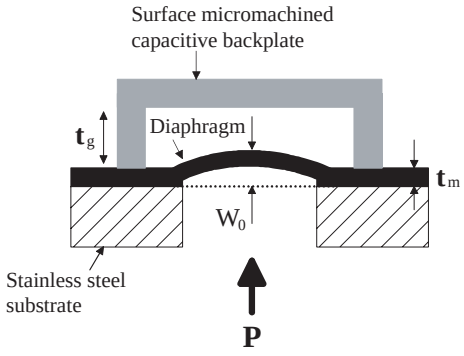

Figure 4. A schematic diagram of the side view of the capacitive pressure sensor.

neglected, since the gap between the flexible diaphragm and the fixed backplate is small compared to their lateral extents; (d) residual stress in the diaphragm can be neglected.

Under these conditions, the deflection of a circular diaphragm with fully clamped perimeter as a function of radius, $w(r)$, is given by [9, 10]

$$w(r) = w_0\left[1 - \left(\frac{r}{a}\right)^2\right]^2 \tag{1}$$

where a is the radius of the plate and w_0 is the center deflection of the plate.

As the electric field fringing effect is neglected under the assumption (c), the electric field lines are perpendicular to the surface of the backplate and the capacitance can be expressed as a function of the shape function $w(r)$ of the membrane by

$$C_s = \varepsilon_0 \int_0^{2\pi} \mathrm{d}\theta \int_0^r \mathrm{d}r \frac{r}{t_\mathrm{g} - w(r)}. \tag{2}$$

We replace $w(r)$ in equation (2) using equation (1) and replace w_0 by the dimensionless parameter

$$\gamma = \frac{w_0}{t_\mathrm{g}}. \tag{3}$$

Then we replace the integration variable r by the dimensionless variable

$$x = \sqrt{\gamma}\left[1 - \left(\frac{r}{a}\right)^2\right]. \tag{4}$$

This yields

$$C = \varepsilon_0 \frac{\pi a^2}{t_\mathrm{g}} \gamma^{-0.5} \int_0^{\sqrt{\gamma}} \frac{\mathrm{d}x}{1 - x^2}. \tag{5}$$

Finally, we solve the integral and use the capacitance when the membrane is undeflected

$$C_0 = \varepsilon_0 \frac{\pi a^2}{t_\mathrm{g}} \tag{6}$$

which yields

$$C = C_0 \gamma^{-0.5} \tanh^{-1}(\gamma^{0.5}) \approx C_0\left(1 + \frac{\gamma}{3} + \frac{\gamma^2}{5}\right) \tag{7}$$

where the second part of equation (7) was obtained from the fifth-order Taylor series expansion of $\tanh^{-1}(y)$.

4. Raw capacitance characterization results

In order to characterize the capacitance of individual pressure sensors, measurements were carried out with a Keithley 3322 LCZ meter. The sensor device to be tested was mounted and sealed on a test fixture. The fixture was connected to a commercial pressure sensor (Fluke Corp. PV 350 Digital Pressure/Vacuum Module) and a digital multimeter to monitor the differential pressure. A compressed nitrogen line was connected to the fixture to serve as the pressure source with a regulator between them to control the differential pressure that would be applied to the fabricated devices. The LCZ meter was then connected to the fabricated sensors to obtain the characterization data for the capacitive pressure sensor.

After collection of the capacitance data, to measure the membrane deflections directly, the electroplated NiFe over the membrane was removed and the exposed membrane was then placed on a microscope stage. Pressure was then applied to the membranes through the fixtures and the resultant deflection of the membrane was observed and measured with the microscope, by measuring with a z-axis micrometer. It is necessary to constantly adjust the microscope head to keep the deflected diaphragm in focus. The test setup is shown in figure 5. By adjusting the input pressure and the focus position, the center deflection of the diaphragm could be measured to a resolution of $\pm 0.4\ \mu$m.

Capacitance versus pressure data of the stainless steel diaphragm based capacitive pressure sensor is shown in

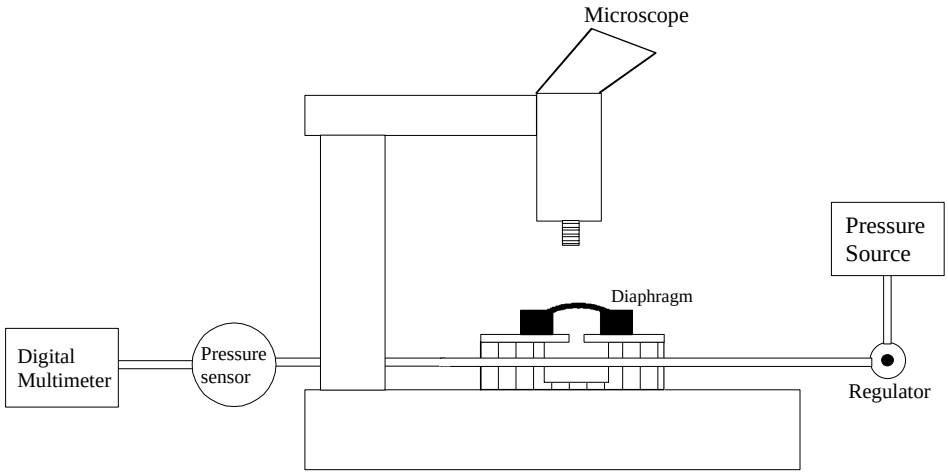

Figure 5. Optical diaphragm deflection measurement setup.

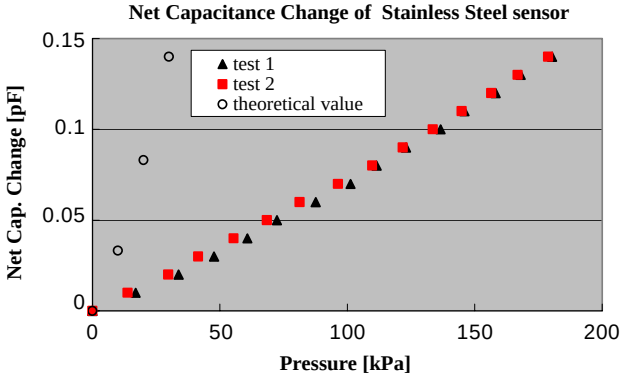

Figure 6. Net capacitance change versus pressure for capacitive pressure sensors.

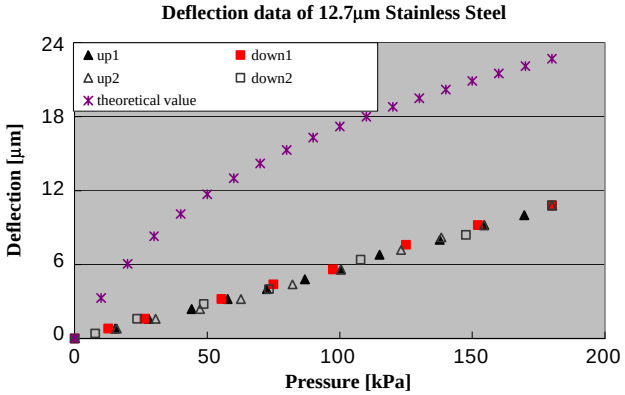

Figure 7. Stainless steel diaphragm deflection versus pressure.

figure 6. For a range of applied pressure from 0 to 178 kPa, the net capacitance change was 0.14 pF. The sensitivities of the sensors were approximately 9.03 ppm kPa^{-1}.

The electromechanical model did not predict the behavior of the sensor well. In order to determine whether the electrical or the mechanical behavior was deviating from the theoretical predictions, the center deflection of the diaphragm as a function of pressure was measured directly. These measurements were performed by removing the sensor backplates upon completion of the capacitance measurements, repeating the pressurization, and observing in a microscope the extent of lateral deflection due to the applied pressure. The deflection data for the stainless steel diaphragm are shown in figure 7, where up1 refers to data from a sample diaphragm under increasing pressure and down1 refers to data from the same diaphragm under decreasing pressure. Up2 and down2 refer to similar data from a second diaphragm.

As can be seen from figure 7, the mechanical model predictions overestimate the measured diaphragm deflections significantly. It is unlikely that the discrepancy is attributable to simple mechanical yielding as identical deflection results were obtained during a pressurization and depressurization cycle. The other assumptions in the model were zero residual stress and isotropic material properties. Finite element calculations predict the presence of significant amounts of residual stress in the film due to cooling from the lamination temperature. The maximum stress in the diaphragm is around 446 MPa including estimated residual stress with 328 MPa in the pressure range 0–180 kPa. The laminated stainless steel diaphragm is still endurable because its yield and ultimate stress are 965 MPa and 1.28 GPa, respectively. In addition, the metallic diaphragms may have anisotropic characteristics due to the rolling and drawing processes used in their manufacture, as well as strains induced during the lamination process.

To verify that the electrical portion of the modeling was correct the measured deflections shown in figure 7 were combined with equations (3) and (7) to yield a prediction of the capacitance of the sensor as a function of pressure. Figure 8 indicates the capacitance versus deflection for the stainless steel diaphragm. The deflection was measured for all cases and the capacitance indicates measured and theoretical values.

As can be seen, the two sets of plots correspond well with each other. This indicates that given the correct deflection data, the calculated capacitance will match up with the measured capacitance.

5. Capacitance read-out circuitry

Two different stages were undertaken in the development of the read-out circuitry for the capacitance pressure microsensors.

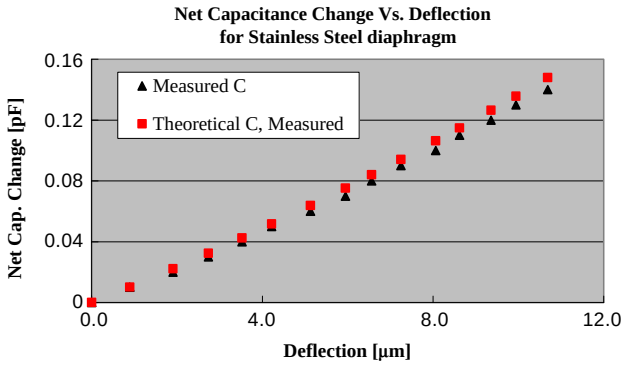

Figure 8. Net capacitance change versus deflection of capacitive pressure sensor.

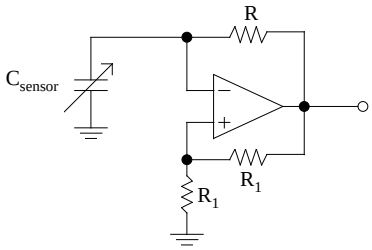

Figure 9. Schematic diagram of an astable multivibrator circuit.

The first stage involved the creation of a simple capacitance-to-frequency conversion circuit to directly read the capacitance changes due to applied pressure. The second stage involved the use of a commercially available MS3110 universal capacitive read-out IC in its un-packaged, die-form from Microsensors, Inc. This chip in its die-form was then integrated via wirebonding to the microfabricated sensors.

5.1. Basic capacitance-to-frequency conversion circuitry

Initially, an op-amp-based astable multivibrator circuit was created in-house to serve as the read-out circuitry for capacitive pressure sensors. This was then integrated with the pressure sensors in a hybrid fashion to create a frequency-modulated voltage output. Figure 9 shows a schematic diagram of such an astable multivibrator circuit, which consists of an LF351 operational amplifier, and three external resistors [11].

The capacitance of the pressure sensor is equivalent to the frequency-determining capacitance that modulates the frequency of the voltage output of the amplifier. The output frequency of the op-amp is given by

$$f = \frac{1}{2RC_{sensor} \ln 3} \tag{8}$$

where RC_{sensor} is the time constant of the circuitry. In this work, external resistors R and R_1 have been selected as 1 MΩ for all three types of pressure sensors.

For this type of sensor, the base frequency was found to be 4081.8 Hz for the output of the op-amp. Figure 10 shows the frequency output of the op-amp circuit as a function of applied pressure from 0 to 180 kPa. The measured value of relative frequency change is 0.2% over the applied pressure range 0–180 kPa. This sensor contained a gap of 27 μm and a sensitivity of 44.8 mHz kPa^{-1}.

5.2. Capacitance-to-voltage conversion circuitry using the MS3110 IC

The values of capacitance and/or corresponding frequency change produced by the sensors are easily measurable in their current form; however, in order to achieve higher sensitivity, elimination of parasitic capacitance is essential. Primary sources of parasitic capacitance include capacitance between bonding pads and substrates, and capacitance between interconnection lines and substrates. Parasitic capacitance from those primary sources can be eliminated by using integrated on-chip circuitry that has a reference electrode, which has the same length of interconnection line and same structure as that of a pressure sensor with a pressure insensitive (immovable) circular plate.

In order to facilitate the use of this improved on-chip circuitry, a commercially available MS3110 universal capacitive read-out IC was used as the read-out circuit [12]. The MS3110 senses the difference between two capacitors and outputs a voltage proportional to the difference. The output voltage can be described by a function of the sensing capacitances $CS1_T$ and $CS2_T$, as shown by the following

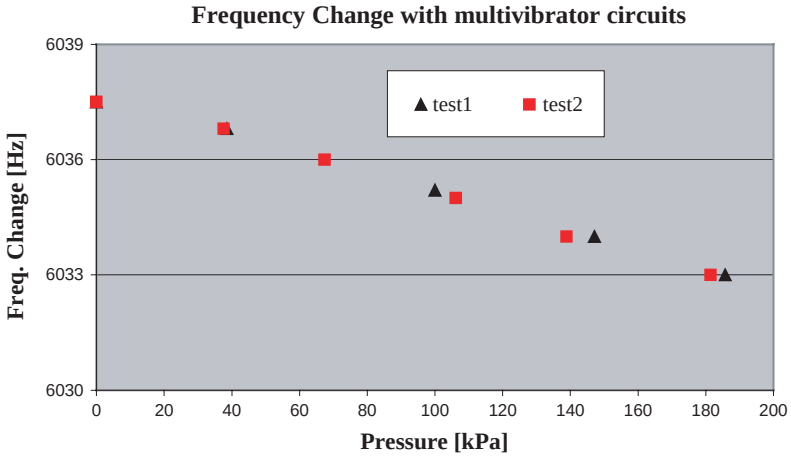

Figure 10. The frequency output of the op-amp circuit as a function of applied pressure from 0 to 180 kPa for the stainless steel pressure sensor.

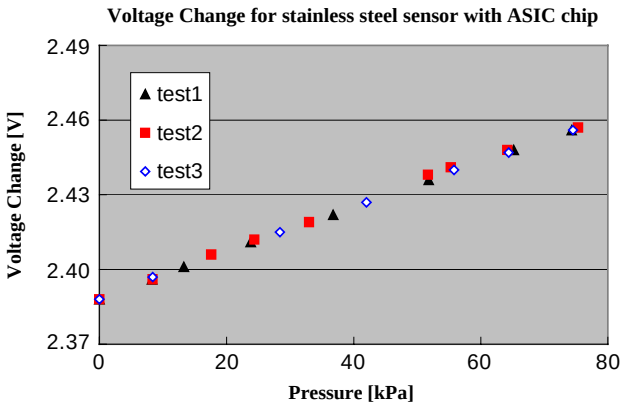

Figure 11. The voltage output of the MS3110 IC for the capacitive pressure sensor.

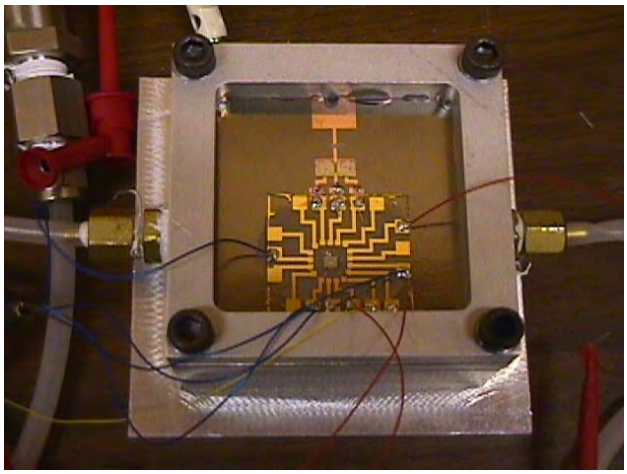

Figure 12. The experimental test setup used in evaluating the sensors using the MS3110.

expression:

$$V_0 = \text{Gain} \times V2P25 \times 1.14 \times \frac{(\text{CS2}_\text{T} - \text{CS1}_\text{T})}{\text{CF}} + V_{\text{ref}} \qquad (9)$$

where $V2P25$ is reference input voltage, which is DC 2.25 V, CS2_T is the input from the microsensor being tested and CS1_T is the reference value as input from the reference microsensor.

Stage 2 of the read-out circuitry involved the use of a die-type MS3110 IC chip that was manually integrated with a microfabricated capacitive pressure sensor. The chip was first mounted on a glass substrate patterned with gold traces for its 15 pads to be used in wirebonding to the pressure sensors built on the stainless steel robust substrate. This was done separately because the substrate field around the sensor was coated with a thin film of SU-8 2 epoxy for insulation ($\sim$6 μm).

This proved to be problematic during the wirebonding process because the ultrasonic technique used in the bonding process served to disturb and destroy adhesion of the epoxy layer on which the bonding pads for the chip were fabricated. By using a separate glass substrate for the IC, the integrity of the insulating epoxy layer was preserved during the wirebonding process. This can be easily connected in future process iterations.

Figure 11 shows the voltage output of the MS3110 for the stainless steel diaphragm sensor as a function of applied pressure from 0 to 75 kPa. The measured value of relative voltage change is 2.85% over the applied pressure range 0–75 kPa. This sensor contained a gap of 21 μm and a sensitivity of 0.92 mV kPa^{-1}.

Figure 12 shows the experimental test setup used in evaluating the sensors using the MS3110.

6. Conclusions

Stainless steel has been studied as a robust substrate and diaphragm material for micromachined devices. Lamination combined with traditional micromachining processes has been investigated as suitable fabrication methods for this robust substrate.

A capacitive pressure sensor has been designed, fabricated, and characterized by using lamination processing with stainless steel films as a diaphragm on the stainless steel shim stock substrate. This sensor has a sensitivity of 9.03 ppm kPa^{-1} with a net capacitance change of 0.14 pF over a range 0–178 kPa.

To avoid the parasitic capacitance, two types of read-out circuitry were introduced to microfabricated sensors. Three different stages were undertaken in the development of the read-out circuitry for the capacitance pressure microsensors.

In the first stage, a simple capacitance-to-frequency conversion circuit was created to read the capacitance changes due to applied pressure. The capacitive pressure sensor utilizing a stainless steel diaphragm gave a sensitivity of 44.8 mHz kPa^{-1} over the applied pressure range 0–180 kPa.

In the second stage, the MS3110 IC in its un-packaged, die-type was integrated via wirebonding to the microfabricated sensors. The measured value of relative voltage change was 2.85% over the applied pressure range 0–75 kPa. This sensor contained a gap of 21 μm and had a sensitivity of 0.92 mV kPa^{-1}.

Acknowledgments

The authors would like to acknowledge Martin von Arx and Guang Yuan for their assistance in the modeling and simulation of the device. The support of the staff of the Microelectronics Research Center and GTRI Machine Shop at Georgia Tech is acknowledged. This work was supported by Defense Advanced Research Project Agency (DARPA) and the Air Force Office of Scientific Research (AFOSR) under contract F49620-97-1-0519.

References

[1] Baltes H 1997 CMOS micro electro mechanical systems *Sensors Mater.* **9** 331–46
[2] MacDonald N C 1996 SCREAM microelectromechanical systems *Microelectron. Eng.* **32** 49–73
[3] Howe R T 1994 Applications of silicon micromachining to resonator fabrication *Proc. 1994 IEEE Int. Frequency Control Symp. (The 48th Annual Symp.)* (Cat. No. 94CH3446–2) pp 2–7
[4] Mastrangelo C H, Zhang X and Tang W C 1995 Surface micromachined capacitive differential pressure sensor with lithographically-defined silicon diaphragm *Proc. Int. Solid-State Sensors and Actuators Conf.—TRANSDUCERS '95 (25–29 June 1995)* vol 1 pp 612–5

[5] Rao R T 2001 *Fundamentals of Microsystems Packaging* (New York: McGraw-Hill)
[6] Stein S J *et al* 1995 Thick film heaters made from dielectric tape bonded stainless steel substrates *Proc. ISHM '95 (Boston, MA)* pp 125–9
[7] Kovacs G T A 1998 *Micromachined Transducers Sourcebook* (New York: McGraw-Hill)
[8] Eaton W P and Smith J H 1997 Micromachined pressure sensors: review and recent developments *Proc. SPIE* **3046** 30–41
[9] Timoshenko S 1940 *Theory of Plates and Shells* (New York: McGraw-Hill)
[10] Ko W H *et al* 1982 A high-sensitivity integrated-circuit capacitive pressure transducer *IEEE Trans. Electron Devices* **29** 48–56
[11] Sedra A S and Smith K C 1982 *Microelectronic Circuits* (New York: CBS College Publishing)
[12] Hsu Y, DeRoo D and Murray J 2001 *Low Cost Sensor for Automotive Applications—The Fabless strategy* (Costa Mesa, CA: Microsensors Inc.)